

Supplementary material

In addition to the results presented in the main body of the paper, we provide a supplementary collection of figures on the fits used in determining the double-tag yields in the two tag modes, and a table summarizing the systematic uncertainties of the partial BFs of $D_s^+ \rightarrow \pi^+\pi^+\pi^-X$ in intervals of $M(\pi^+\pi^+\pi^-)$.

Table 1: Summary of all different sources of systematic uncertainties for partial branching fractions of $D_s^+ \rightarrow \pi^+\pi^+\pi^-X$. The uncertainties are summed up in quadrature to make the total systematic uncertainties.

| Source | Relative uncertainty (%) in $M(\pi^+\pi^+\pi^-)$ interval | | | | | | | | | | |
|--------------|---|------|------|------|------|------|------|------|------|------|------|
| | 1 | 2 | 3 | 4 | 5 | 6 | 7 | 8 | 9 | 10 | 11 |
| Sig. shape | 0.70 | 1.73 | 0.49 | 0.86 | 1.84 | 2.62 | 2.55 | 2.41 | 1.55 | 1.56 | 0.17 |
| Bkg. shape | 0.04 | 0.42 | 0.04 | 0.33 | 0.68 | 0.63 | 0.09 | 0.20 | 1.28 | 0.65 | 0.15 |
| Track eff. | 2.44 | 1.73 | 1.34 | 0.96 | 0.72 | 0.50 | 0.37 | 0.19 | 0.01 | 0.17 | 0.43 |
| PID eff. | 0.77 | 1.26 | 0.95 | 0.87 | 0.68 | 0.50 | 0.23 | 0.19 | 0.39 | 0.71 | 0.59 |
| K_S^0 bkg. | 0.30 | 0.64 | 0.58 | 0.40 | 0.29 | 0.24 | 0.17 | 0.19 | 0.19 | 0.06 | 0.02 |
| Kaon misID | 0.40 | 0.49 | 0.42 | 0.36 | 0.30 | 0.23 | 0.17 | 0.14 | 0.19 | 0.28 | 0.02 |
| Lepton misID | 0.28 | 0.45 | 0.37 | 0.35 | 0.38 | 0.34 | 0.31 | 0.37 | 0.44 | 0.25 | 0.02 |
| Pion mult. | 0.91 | 1.12 | 1.11 | 0.73 | 0.39 | 0.19 | 0.01 | 0.15 | 0.33 | 0.06 | 0.00 |
| Pion mom. | 0.46 | 1.84 | 1.26 | 1.75 | 1.30 | 1.08 | 0.90 | 0.65 | 0.14 | 0.79 | 2.80 |
| MC size | 0.32 | 0.30 | 0.39 | 0.41 | 0.61 | 0.51 | 0.61 | 0.55 | 0.67 | 0.63 | 1.45 |
| Fit bias | 0.90 | 1.24 | 0.77 | 0.08 | 0.38 | 0.45 | 0.93 | 0.57 | 0.15 | 0.81 | 2.57 |
| Total | 3.05 | 3.86 | 2.68 | 2.59 | 2.74 | 3.11 | 2.99 | 2.68 | 2.25 | 2.29 | 4.14 |

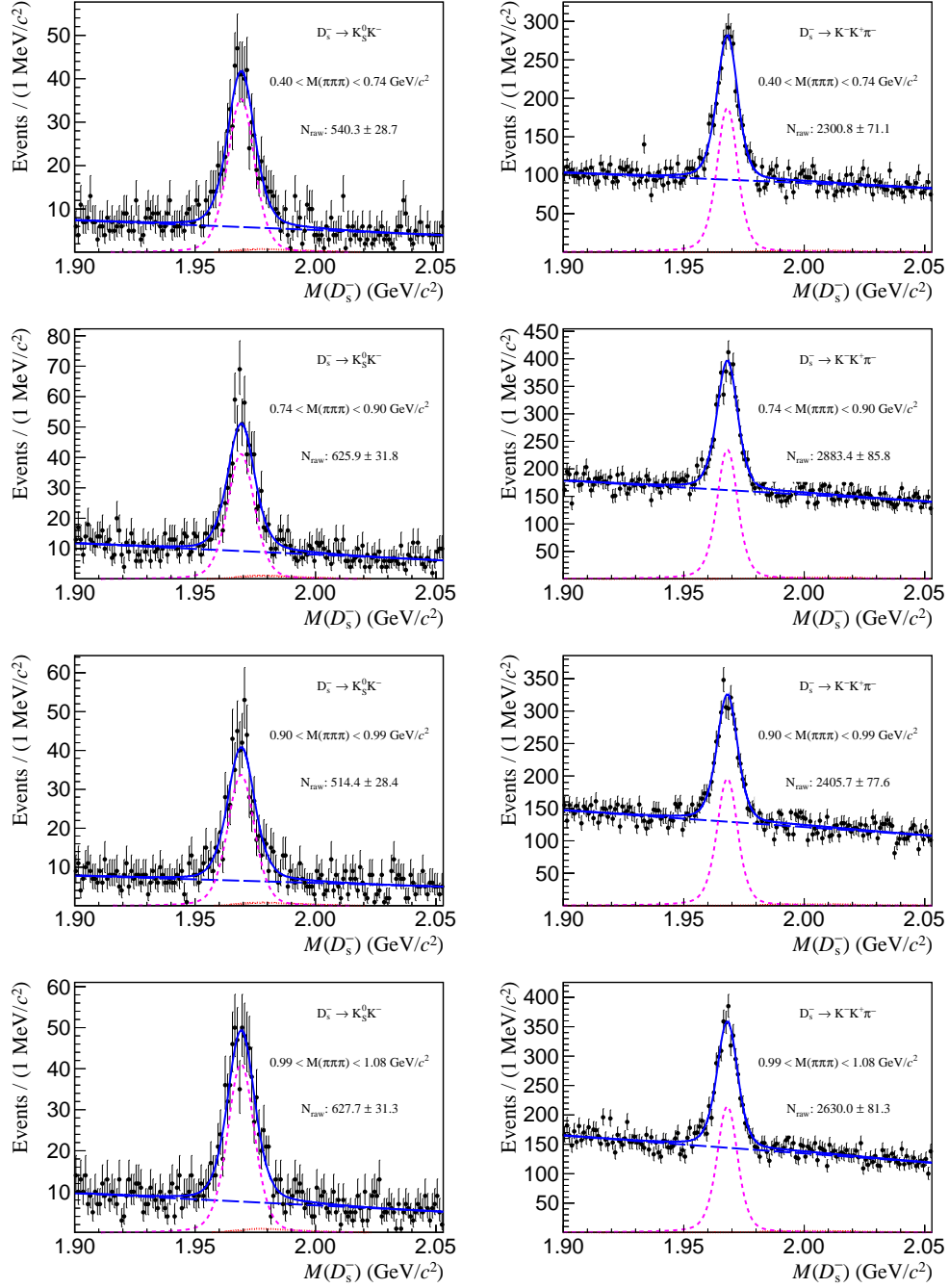


Figure 1: The invariant mass $M(D_s^-)$ distributions for the ST modes $D_s^- \rightarrow K_S^0 K^-$ (left) and $D_s^- \rightarrow K^- K^+ \pi^-$ (right), part 1/3. Data (black points) are shown overlaid with the fit results including the total (solid blue), signal PDF (dashed magenta), D^- background PDF (dotted red), and combinatorial background PDF (long-dashed blue) components.

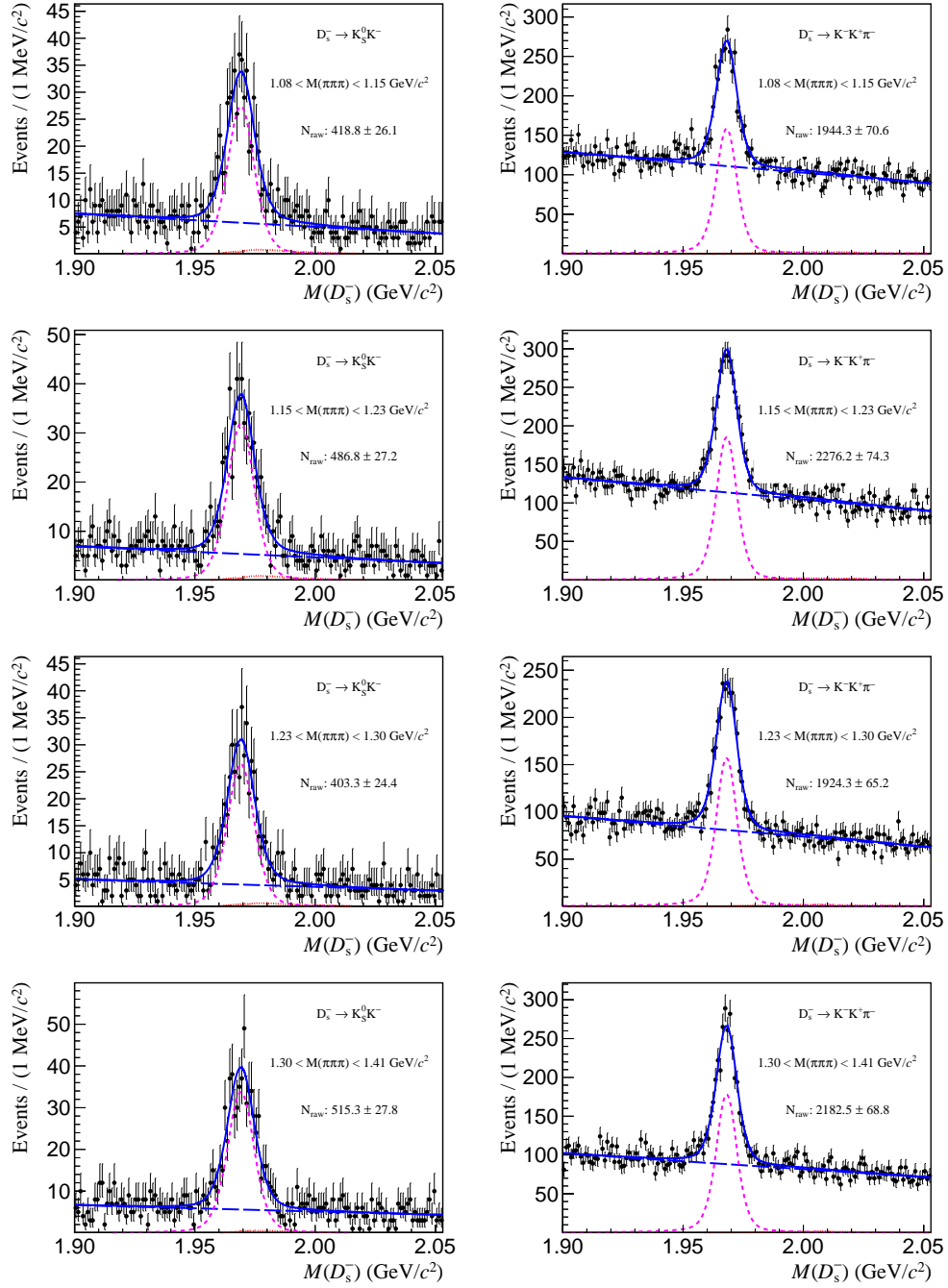


Figure 2: The invariant mass $M(D_s^-)$ distributions for the ST modes $D_s^- \rightarrow K_S^0 K^-$ (left) and $D_s^- \rightarrow K^- K^+ \pi^-$ (right), part 2/3. Data (black points) are shown overlaid with the fit results including the total (solid blue), signal PDF (dashed magenta), D^- background BDF (dotted red), and combinatorial background PDF (long-dashed blue) components.

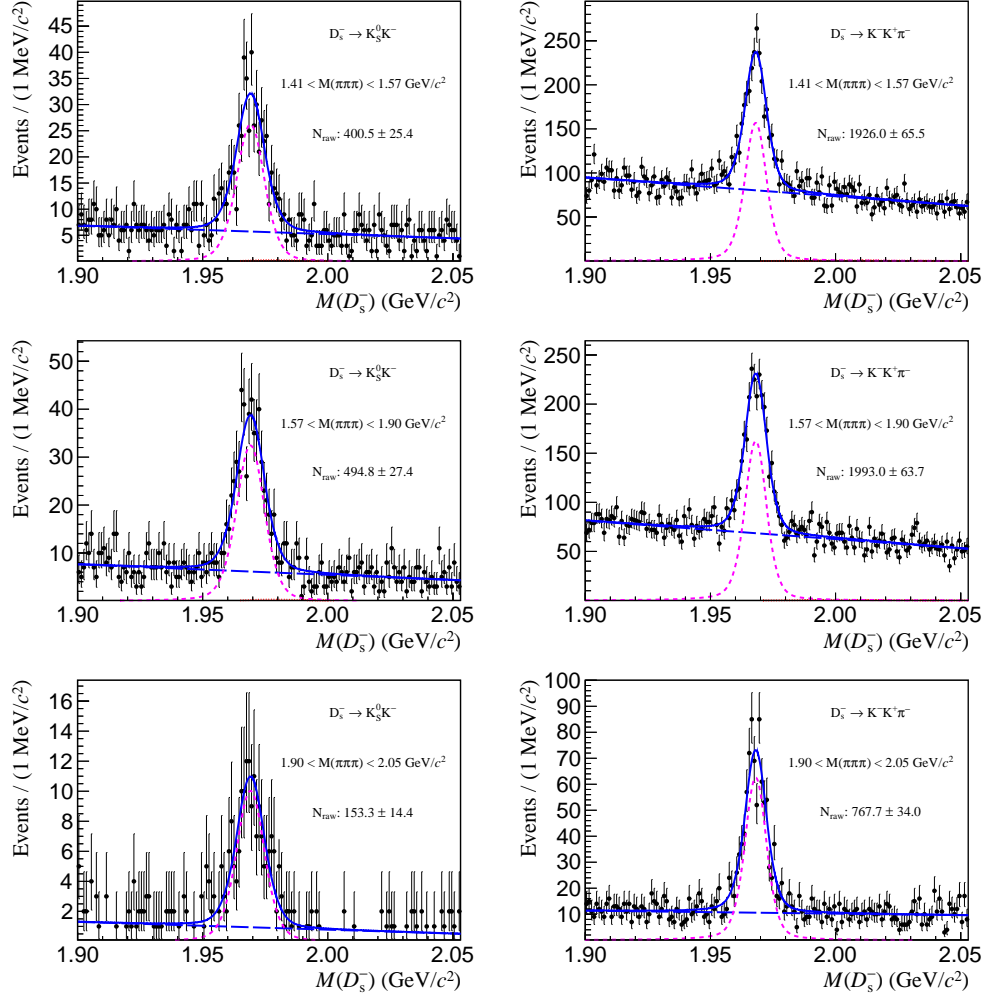


Figure 3: The invariant mass $M(D_s^-)$ distributions for the ST modes $D_s^- \rightarrow K_S^0 K^-$ (left) and $D_s^- \rightarrow K^- K^+ \pi^-$ (right), part 3/3. Data (black points) are shown overlaid with the fit results including the total (solid blue), signal PDF (dashed magenta), D^- background PDF (dotted red), and combinatorial background PDF (long-dashed blue) components.